Characterization of a Compton camera setup with monolithic $LaBr_3$(Ce) absorber and segmented GAGG scatter detectors

Liprandi, Silvia; Takyu, Sodai; Aldawood, Saad; Binder, Tim; Dedes, George; Kamada, Kei; Lutter, Rudolf; Mayerhofer, Michael; Schaart, Dennis R.; More Authors

DOI
10.1109/NSSMIC.2017.8533134

Publication date
2018

Document Version
Final published version

Published in
2017 IEEE Nuclear Science Symposium and Medical Imaging Conference, NSS/MIC 2017 - Conference Proceedings

Characterization of a Compton camera setup with monolithic $LaBr_3(Ce)$ absorber and segmented GAGG scatter detectors

Silvia Liprandi, *IEEE Student Member*, Sodai Takyu, Saad Aldawood, Tim Binder, George Dedes, Kei Kamada, Rudolf Lutter, Michael Mayerhofer, Agnese Miani, Akram Mohammadi, *IEEE Member*, Fumihiko Nishikido, Dennis R. Schaart, *IEEE Member*, Ingrid I. Valencia Lozano, Eiji Yoshida, Taiga Yamaya, *IEEE Member*, Katia Parodi, *IEEE Member*, and Peter G. Thirolf

***Abstract*–The purpose of this study is to perform a first characterization and proof of principle investigation of a Compton camera setup composed by a scatterer component consisting of a pixelated GAGG crystal read out by a SiPM multi-pixel photon counter (MPPC) and an absorber component consisting of a monolithic $LaBr_3(Ce)$ scintillator read out by a 256-fold multianode photomultiplier (PMT). The rationale of the study is to develop a Compton camera system as a future ion beam range verification device during particle therapy, via prompt gamma imaging. The properties to be investigated are the reconstruction efficiency and accuracy achievable with this system for detecting prompt-γ rays. The Compton camera system described has been tested with a laboratory radioactive Cesium-137 source, in a certain geometrical configuration. The readout system is based on individual spectroscopy (NIM+VME) electronic modules, digitizing energy and time signals. The data have been analyzed to produce an input for the image reconstruction, performed using the MEGAlib toolkit software.**

I. Introduction

PARTICLE beam therapy is nowadays considered an advantageous option in cancer treatment, but the beneficial high dose delivery precision on the other hand demands a high accuracy of the Bragg peak placement: different approaches for the beam range monitoring are worldwide being evaluated.

Manuscript received November 10, 2017. This work is supported by the NIRS International Open Laboratory, the DFG Cluster of Excellence Munich Centre for Advanced Photonics (MAP), King Saud University (KSU).

S. Liprandi is with the Department of Medical Physics, Ludwig Maximilian University, Munich, Germany (Silvia.Liprandi@physik.uni-muenchen.de).

S. Takyu, A. Mohammadi, F. Nishikido, E. Yoshida, T. Yamaya are with the National Institute of Radiological Sciences (NIRS) at National Institutes for Quantum and Radiological Science and Technology (QST), Chiba, Japan.

T. Binder, G. Dedes, R. Lutter, I.I. Valencia Lozano, K. Parodi, P.G. Thirolf are with the Department of Medical Physics, Ludwig Maximilian University, Munich, Germany.

S. Aldawood is now with the Department of Physics and Astronomy, King Saud University, Riyadh, Saudi Arabia. He was with the Department of Medical Physics, Ludwig Maximilian University, Munich, Germany.

M. Mayerhofer is now with the Department of Physics, Universität der Bundeswehr, Munich, Germany. He was with the Department of Medical Physics, Ludwig Maximilian University, Munich, Germany and the Department of Physics, University of Hamburg, Hamburg, Germany.

A. Miani is now with Cambridge Medical Robotics Ltd., Cambridge, UK. She was with the Department of Medical Physics, Ludwig Maximilian University, Munich, Germany.

D.R. Schaart is with Delft University of Technology, Delft, The Netherlands.

K. Kamada is with C&A corporation, Sendai, Japan.

978-1-5386-2282-7/17/$31.00 ©2017 IEEE

The Compton camera is one of the proposed techniques, which aims at providing real-time, in-vivo proton (or ion) beam range monitoring by means of detection of secondary prompt gamma rays [1].

From the Compton kinematics, an image of the prompt gamma source position can be reconstructed, which is directly correlated to the particle beam range (Fig. 1).

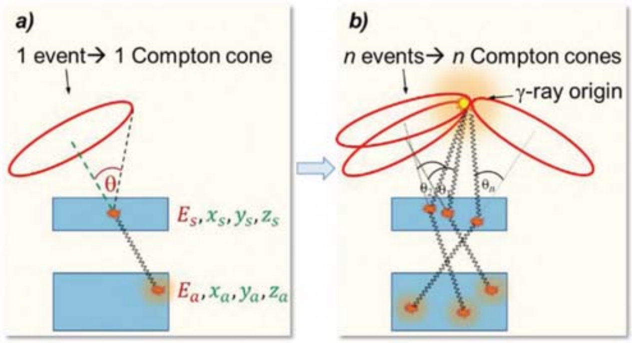

Fig. 1. Sketch of the image reconstruction process using a Compton camera system, composed of a scatterer and an absorber component. *a)* Compton scattering of an incident photon, where energies and positions are recorded in each of the two detector components, the scatterer and the absorber. Via the Compton kinematics, the Compton cone can be reconstructed: the energy and position information allows, respectively, to determine its axis and its aperture angle (scattering angle θ). b*)* The intersection of different cones reconstructed from all the different photon events allows to reconstruct the photon source position, corresponding to the interaction position of the proton / ion beam in the patient.

The purpose of this work is the characterization of a detector system composed of a pixelated GAGG scintillation detector array coupled to an MPPC SiPM array acting as scatterer component and a monolithic $LaBr_3(Ce)$ scintillator read out by a multi-anode photomultiplier (PMT) acting as absorber component, in a defined Compton camera setup geometry.

II. Materials and Methods

In the study presented here, we have acquired and analyzed data from a Compton camera setup tested at a photon energy of $E_\gamma = 662$ keV from an uncollimated ^{137}Cs point source.

The camera consists of a segmented array of 22x22 individual GAGG ($Gd_3Al_2Ga_3O_{12}(Ce)$) crystals (each

0.9x0.9x6 mm³) coupled to an MPPC SiPM array (Hamamatsu S13361-3050AE-08, 8x8 ch, 3584 pixels/ch) acting as scatterer and a monolithic $LaBr_3(Ce)$ scintillator, read out by a 256-fold segmented multi-anode photomultiplier (PMT H9500 Hamamatsu), acting as absorber, the latter chosen due to its excellent energy and time resolution, demonstrated at LMU Munich in dedicated studies [2, 3].

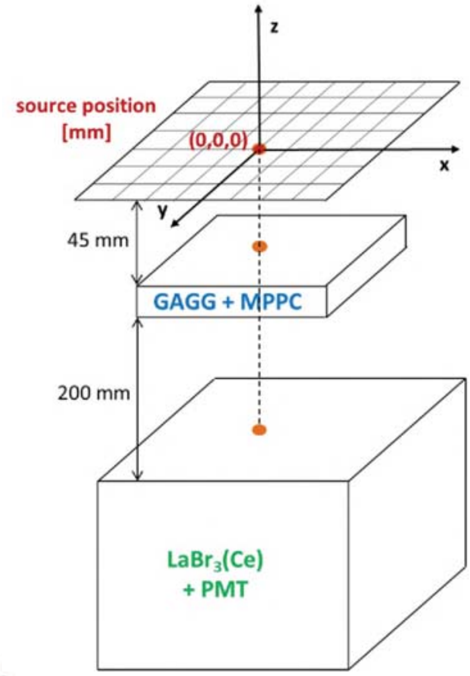

Fig. 2. Sketch of the Compton camera setup: the GAGG and $LaBr_3(Ce)$ detectors were placed in a distance of 200 mm. The ^{137}Cs source was placed in a distance of 45 mm from the scatterer component in a central position on the (x,y) plane: (0,0,0) [mm] in the coordinate system of the setup.

The two detectors were placed in a relative distance of 200 mm, and the ^{137}Cs source was placed in the center at 45 mm from the scatterer component (see Fig. 2).

The data acquisition was performed using a PowerPC (RIO) in a VME crate and the Marabou software [9].

The signal processing of the GAGG array was performed with a customized electronics, providing 4 output signals and a sum signal, thus enabling the Anger logic calculation for position determination.

The 5 signals from the GAGG detector and the 256 channels of the PMT coupled to the monolithic $LaBr_3(Ce)$ scintillator together with its sum dynode output were readout using CFD and QDC (charge digitizer) modules [6, 7].

Thresholds were applied to the signals in the CFD modules and corrections were applied: gain matching, pedestal cut, PMT non-uniformity.

The position determination in the monolithic $LaBr_3(Ce)$ crystal was performed using the k-Nearest-Neighbors (kNN) algorithm [3, 4], in particular the Categorical Average Pattern (CAP) variation of the algorithm (see the principle of the algorithm in Fig. 3).

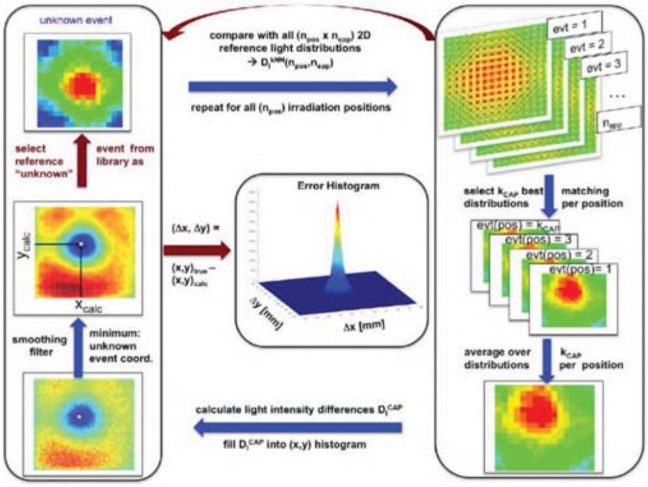

Fig. 3. Workflow chart of the CAP version of the kNN algorithm for extracting the interaction position of an unknown impinging gamma ray in the monolithic $LaBr_3(Ce)$ scintillator, in this case taken from a reference library to quantify the spatial resolution from the FWHM (Full Width Half Maximum) of the error histogram created from deviations between real and calculated photon interaction positions.

The Compton camera performance was evaluated for the geometrical configuration presented in this record.

The Compton-scattered events were chosen using the coincidences between scatterer and absorber, discarding events with unphysical calculated scattering angles according to (1)

$$\cos\theta = 1 - m_e c^2 \left(\frac{1}{E_{abs}} - \frac{1}{E_{abs} + E_{scatt}} \right)$$

$$0 < m_e c^2 \left(\frac{1}{E_{abs}} - \frac{1}{E_{abs} + E_{scatt}} \right) < 1 \qquad (1)$$

where E_{abs} and E_{scatt} refer to the energy deposited in the absorber and scatterer components, θ is the Compton scattering angle of the gamma ray and m_e is the electron mass.

As a benchmarking study, simulated data were also produced using the same geometrical configuration.

The photon source image reconstruction was based on the List-Mode Maximum-Likelihood Expectation-Maximization (LM-ML-EM) [10] algorithm, giving the position and energy information of the selected events from both detectors as an input to the MEGAlib toolkit software [8]. A quantitative evaluation was based on the calculation of the standard deviation (σ) and source position, fitted according to a 2D Gaussian model.

III. RESULTS

From all the events acquired during the measurement (using the $LaBr_3(Ce)$ sum signal as trigger), we selected only Compton-scattered events, i.e. coincidences between scatterer and absorber, for the subsequent interaction position determination and source image reconstruction. A corresponding gate condition was defined, above the detectors' noise level, in the 2D $E_{scatter}$ vs $E_{absorber}$ plane, as shown in Fig. 4.

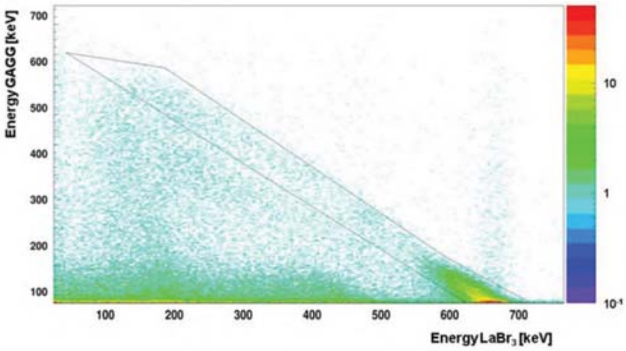

Fig. 4. Registered sum energy in the GAGG detector array (scatterer) versus the sum energy registered in the LaBr$_3$(Ce). The black trapezoid encloses the coincident Compton scattering events selected as the data basis for the subsequent reconstruction calculations.

The data selected to be part of the Compton kinematics calculation were then separately analyzed to obtain the interaction position and energy deposition information from both components of the Compton camera: the data from the GAGG detector array were analyzed based on an Anger logic algorithm, while the position data from the LaBr$_3$(Ce) absorber were derived from the CAP version of the kNN algorithm. In Fig. 5 the position determination in the LaBr$_3$(Ce) scintillator for one event as part of a photon source image reconstruction is exemplified.

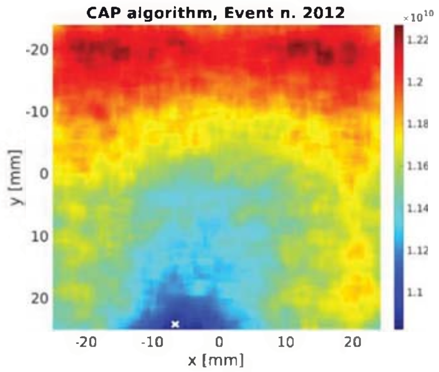

Fig. 5. Example of position reconstruction using CAP algorithm for one event registered in the monolithic LaBr$_3$(Ce) scintillator. The white cross at the lower border indicates the calculated position of the photon source.

The spatial resolution of the monolithic LaBr$_3$(Ce) scintillator at 662 keV was previously [3] determined as 4.8(1) mm, significantly improving at higher energies (2.9(1) mm at 1.3 MeV [5]). Further improvements are expected for the energy range of prompt γ-rays (3-6 MeV), from the observed energy-dependent trend of the calculated spatial resolution [3, 5].

In Fig. 6 the image of the photon source position reconstruction for the GAGG-LaBr$_3$(Ce) Compton setup is depicted, in which the source was placed in a central position on the (x,y) plane and in a distance of 45 mm from the scatterer component (on the z axis). The white cross indicates the nominal position of the photon source. The experimental result was compared to the image reconstructed from simulated data, showing good agreement (Fig. 6a and 6b).

The corresponding fitted σ values and (x,y) source positions are reported in Table 1, for simulated and experimental data, respectively.

Furthermore, the Angular Resolution Measurement (ARM) was calculated to be 5.97° for the simulated data and 13.21° for the experimental data.

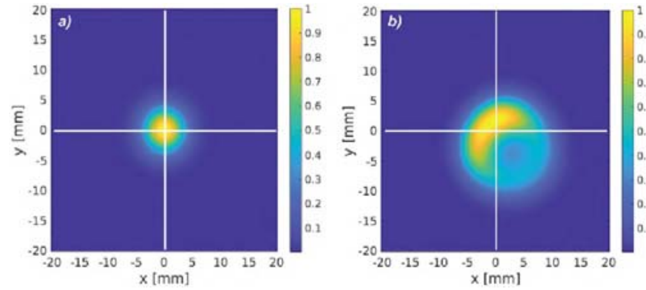

Fig. 6. Reconstructed source position images from *a)* simulated data and *b)* experimental data.

TABLE I. 2D GAUSSIAN FIT

	Simulated data *(a)*	Experimental data *(b)*
Δx [mm]	0.14	-0.34
Δy [mm]	0.16	0.76
σ_x [mm]	4.9	4.9
σ_y [mm]	4.9	7.2
ARM [°]	5.97	13.21

IV. DISCUSSIONS AND CONCLUSIONS

A study for a GAGG-LaBr$_3$(Ce) Compton camera setup is presented, with first laboratory tests including an analysis for the photon source image reconstruction and a benchmarking simulation study.

The photon source position images are based on the intersection of Compton cones defined by the interaction positions and energy depositions in the two detector components and were reconstructed using the MEGAlib toolkit software, based on the LM-ML-EM algorithm. The images obtained were qualitatively and quantitatively evaluated via a fit based on a 2D Gaussian model.

Further measurements in different geometrical scenarios and with higher photon energies will be performed with the presented Compton camera setup, in the direction of a complete proof of principle study in the energy range of interest for prompt gamma rays.

REFERENCES

[1] J. Krimmer, D. Dauvergne, J.M. Létang, and É. Testa, "Prompt-gamma monitoring in hadrontherapy: A review," Nuclear Inst. And Methods in Physics Research, A, 2017.
[2] S. Aldawood, I. Castelhano, R. Gernhäuser, H. Van Der Kolff, C. Lang, S. Liprandi, R. Lutter, L. Maier, T. Marinšek, D.R. Schaart, K. Parodi, and P.G. Thirolf, "Comparative characterization study of a LaBr$_3$(Ce) scintillation crystal in two surface wrapping scenarios: Absorptive and reflective," Frontiers and Oncology, 5:270, 2015.
[3] S. Aldawood, P.G. Thirolf, A. Miani, M. Böhmer, G. Dedes, R. Gernhäuser, C. Lang, S. Liprandi, L. Maier, T.Marinšek, M. Mayerhofer, D.R. Schaart, I.I. Valencia Lozano, and K. Parodi,

"Development of a Compton Camera for prompt-gamma medical imaging," Radiation Physics and Chemistry 140C, 190-197, 2017.

[4] Van Dam H.T., S. Seifert, R. Vinke, P. Dendooven, H Löhner, F. J. Beekman, and D.R. Schaart, "Improved Nearest Neighbor Methods for Gamma Photon interaction position determination in monolithic scintillator PET detectors," IEEE Trans. Nucl. Sci. 58: 2139-2147, 2011.

[5] S. Liprandi, M. Mayerhofer, S. Aldawood, T. Binder, G. Dedes, A. Miani, D.R. Schaart, I. I. Valencia Lozano, K. Parodi, and P.G. Thirolf, "Sub-3mm spatial resolution from a large monolithic $LaBr_3$ (Ce) scintillator," Current Directions in Biomedical Engineering 3(2): 655-659, 2017.

[6] Mesytec, Data sheet V1.8_09 MCFD-16 module, http://www.mesytec.com/products/datasheets/MCFD-16.pdf.

[7] Mesytec, Data sheet V1.4_08 MQDC-32 module, http://www.mesytec.com/products/datasheets/MQDC-32.pdf.

[8] A. Zoglauer, R. Andritschke, and F. Schopper, "MEGAlib – The Medium Energy Gamma-ray Astronomy Library," New Astronomy Reviews 50: 629-632, 2006.

[9] R. Lutter, O. Schaile, K. Schöffel, K. Steinberger, P. Thirolf, and C. Broude, "MARaBOU – a MBS and ROOT based Online/Offline Utility," IEEE Trans. Nucl. Sci. 47: 280-283, 2000.

[10] S.J. Wilderman, N. Clinthorne, J. Fessler, and W. Rogers, "List-Mode Maximum Likelihood reconstruction of Compton scatter camera images in nuclear medicine," Nuclear Science Symposium, Conference Record, vol. 3, pp. 1716–1720, IEEE, 1998.